

2013

Use of NMR logging to obtain estimates of hydraulic conductivity in the High Plains aquifer, Nebraska, USA

Katherine Dlubac
Stanford University

Rosemary Knight
Stanford University, rknight@stanford.edu


Yi-Qiao Song
Schlumberger Doll Research

Nate Bachman
Schlumberger Dhahran Carbonate Research

Ben Grau
Schlumberger Water Services

See next page for additional authors

Follow this and additional works at: <http://digitalcommons.unl.edu/usgsstaffpub>

 Part of the [Geology Commons](#), [Oceanography and Atmospheric Sciences and Meteorology Commons](#), [Other Earth Sciences Commons](#), and the [Other Environmental Sciences Commons](#)

Dlubac, Katherine; Knight, Rosemary; Song, Yi-Qiao; Bachman, Nate; Grau, Ben; Cannia, Jim; and Williams, John, "Use of NMR logging to obtain estimates of hydraulic conductivity in the High Plains aquifer, Nebraska, USA" (2013). *USGS Staff -- Published Research*. 1011.

<http://digitalcommons.unl.edu/usgsstaffpub/1011>

This Article is brought to you for free and open access by the US Geological Survey at DigitalCommons@University of Nebraska - Lincoln. It has been accepted for inclusion in USGS Staff -- Published Research by an authorized administrator of DigitalCommons@University of Nebraska - Lincoln.

Authors

Katherine Dlubac, Rosemary Knight, Yi-Qiao Song, Nate Bachman, Ben Grau, Jim Cannia, and John Williams

Use of NMR logging to obtain estimates of hydraulic conductivity in the High Plains aquifer, Nebraska, USA

Katherine Dlubac,¹ Rosemary Knight,¹ Yi-Qiao Song,² Nate Bachman,³ Ben Grau,⁴ Jim Cannia,⁵ and John Williams⁶

Received 31 May 2012; revised 5 February 2013; accepted 14 February 2013; published 15 April 2013.

[1] Hydraulic conductivity (K) is one of the most important parameters of interest in groundwater applications because it quantifies the ease with which water can flow through an aquifer material. Hydraulic conductivity is typically measured by conducting aquifer tests or wellbore flow (WBF) logging. Of interest in our research is the use of proton nuclear magnetic resonance (NMR) logging to obtain information about water-filled porosity and pore space geometry, the combination of which can be used to estimate K . In this study, we acquired a suite of advanced geophysical logs, aquifer tests, WBF logs, and sidewall cores at the field site in Lexington, Nebraska, which is underlain by the High Plains aquifer. We first used two empirical equations developed for petroleum applications to predict K from NMR logging data: the Schlumberger Doll Research equation (K_{SDR}) and the Timur-Coates equation ($K_{\text{T-C}}$), with the standard empirical constants determined for consolidated materials. We upscaled our NMR-derived K estimates to the scale of the WBF-logging $K(K_{\text{WBF-logging}})$ estimates for comparison. All the upscaled $K_{\text{T-C}}$ estimates were within an order of magnitude of $K_{\text{WBF-logging}}$ and all of the upscaled K_{SDR} estimates were within 2 orders of magnitude of $K_{\text{WBF-logging}}$. We optimized the fit between the upscaled NMR-derived K and $K_{\text{WBF-logging}}$ estimates to determine a set of site-specific empirical constants for the unconsolidated materials at our field site. We conclude that reliable estimates of K can be obtained from NMR logging data, thus providing an alternate method for obtaining estimates of K at high levels of vertical resolution.

Citation: Dlubac, K., R. Knight, Y.-Q. Song, N. Bachman, B. Grau, J. Cannia, and J. Williams (2013), Use of NMR logging to obtain estimates of hydraulic conductivity in the High Plains aquifer, Nebraska, USA, *Water Resour. Res.*, 49, 1871–1886, doi:10.1002/wrcr.20151.

1. Introduction

[2] There are several hydrological methods that can be used to obtain estimates of hydraulic conductivity in unconsolidated groundwater aquifers. While these methods can provide valuable insight into the hydraulic conductivity within the investigated zone, many of them also have limitations [Butler, 2005; Chen *et al.*, 2012]. An aquifer test, which is the most common method used in the field to estimate transmissivity and hydraulic conductivity, can be time consuming and expensive, requires one pumping well and at least one observation well, and provides hydraulic conductivity estimates that are averaged over the entire

producing zone of the aquifer. While hydraulic conductivity at this scale may be all that is required to characterize the producing zone of an aquifer, it may not be adequate for identifying vertical heterogeneity within the aquifer, such as thin nonpermeable layers that can affect flow rate and direction. In contaminant investigations, high-resolution hydraulic conductivity estimates are often required to identify layers that affect the transport of a contaminant. Likewise, in aquifer storage and recovery programs, hydraulic conductivity estimates with higher vertical resolution can identify layers that may block infiltration of the recharged water to the desired aquifer location for storage. Other hydrologic methods exist that provide high-resolution hydraulic conductivity estimates; these include slug tests, multilevel slug tests, dipole-flow tests, and wellbore flow (WBF) logging. However, these methods can also be time consuming because at each depth interval, the system must reach equilibrium before the measurement can be made. There are several other limitations to the high-resolution hydrological methods. For example, in order to interpret WBF logging measurements, a transmissivity or hydraulic conductivity estimate obtained through aquifer testing is often required. Likewise, in order to interpret dipole-flow test measurements, a test that estimates the vertical variations in hydraulic conductivity in a single borehole using a three-packer tool [Kabala, 1993; Butler *et al.*, 1998], an estimate of the anisotropy ratio between

¹Geophysics Department, Stanford University, Stanford, California, USA.

²Schlumberger Doll Research, Cambridge, Massachusetts, USA.

³Schlumberger Dhahran Carbonate Research, Dhahran, Saudi Arabia.

⁴Schlumberger Water Services, Tucson, Arizona, USA.

⁵Nebraska Water Science Center, U.S. Geological Survey, Lincoln, Nebraska, USA.

⁶Office of Groundwater-Branch of Geophysics, U.S. Geological Survey, Troy, New York, USA.

Corresponding author: R. Knight, Geophysics Department, Stanford University, Stanford, CA 94305-2215, USA. (rknight@stanford.edu)

vertical and radial hydraulic conductivity, is required. Other methods have a more direct interpretation but may provide less reliable estimates. An example of this is the hydraulic conductivity estimate derived from slug tests, which can be highly dependent on the construction and development of the well [Butler, 1998]. Additionally, because each test predicts hydraulic conductivity through a different technique, it is not uncommon for the resulting hydraulic conductivity estimates to vary between methods. Within a single type of test, because of assumptions and variations in acquisition parameters, it is not uncommon for hydraulic conductivity estimates to vary by an order of magnitude. An order of magnitude variation is considered acceptable for purposes of aquifer characterization and assessment.

[3] In this study we examined the ability of proton nuclear magnetic resonance (NMR) borehole logging to provide reliable hydraulic conductivity estimates in aquifers. Hydraulic conductivity estimates obtained from NMR logging data have advantages over traditional hydrological methods in that only one borehole is required, the measurements have high vertical resolution, and data acquisition is generally less time consuming than other hydrological methods. Additionally, with the recent development of a slimhole NMR logging tool, data can be collected in existing pumping and observation wells that have been completed with PVC casing [Walsh *et al.*, 2010].

[4] NMR logging is widely used in oil and gas reservoirs in the petroleum industry as a means of estimating permeability, which is related to hydraulic conductivity through the fluid properties. The technology has undergone significant technological advancements over the past two decades. Collecting NMR logging measurements involves lowering a tool into a borehole to record the response of the nuclear magnetization associated with the hydrogen nuclei in the pore fluids (oil, water, and gas) of the geologic materials directly surrounding the borehole. The NMR measurement involves perturbing the system from equilibrium and then recording the change in magnetization as the system returns to equilibrium. The time-dependent change in magnetization contains information about the porosity and geometry of the water-filled regions of the pore space. There are two relationships commonly used to obtain estimates of permeability from this NMR-derived information [SeEVERS, 1966; TIMUR, 1968; KENYON *et al.*, 1988; COATES *et al.*, 1991b]: the Schlumberger Doll Research (SDR) and the Timur-Coates (T-C) equations, both of which require empirically determined constants. A set of standard empirical constants have been determined through laboratory studies on consolidated materials and have been found to yield reliable estimates of permeability in reservoir materials [COATES *et al.*, 2000; DUNN, 2002; ELLIS and SINGER, 2007], thus establishing NMR logging as a highly valued method for petroleum applications. The motivating question in our research: Can NMR logging be used, with these same relationships, to estimate hydraulic conductivity in near-surface unconsolidated groundwater aquifers?

[5] The few studies that have utilized NMR logging to obtain permeability estimates for groundwater applications have been conducted in consolidated sandstone and carbonate aquifers [LEWIS *et al.*, 2000; PARRA *et al.*, 2003; MALIVA *et al.*, 2009]. In these studies, permeability estimates were

obtained using the SDR and/or T-C relationships with the standard empirical constants. It was reasonable to use the standard constants in these studies, given that they were determined using consolidated materials. Unfortunately, these studies do not provide any other measurements of permeability, which makes it impossible to assess the accuracy of NMR-derived permeability estimates.

[6] A study in an unconsolidated petroleum reservoir found that permeability predicted using the SDR and T-C relationships with the standard empirical constants resulted in predictions that were several orders of magnitude lower than the permeability values measured on the core samples [HODGKINS and HOWARD, 1999]. By calibrating the logging data with the core measurements to obtain calibrated empirical constants, more reliable NMR-derived permeability estimates were obtained; unfortunately, the values for the calibrated empirical constants were not reported.

[7] In this study, we investigated the ability of NMR logging measurements to provide reliable estimates of hydraulic conductivity in an unconsolidated aquifer. Our field site for this study was in Lexington, Nebraska, which is underlain by the High Plains aquifer. We first predicted NMR-derived hydraulic conductivity using the SDR and T-C equations with the standard empirical constants. We compared these predictions to hydraulic conductivity estimates obtained from WBF logging. We then calibrated the SDR and T-C equations to determine a set of empirical constants for the unconsolidated materials at our field site.

2. Background

2.1. NMR Relaxation Theory

[8] The NMR phenomenon was first discovered in 1945 when it was observed that atoms with an odd number of protons or neutrons possess a magnetic moment and a nuclear spin angular momentum, and thus are able to absorb and transmit energy when disturbed from equilibrium [BLOCH, 1946; PURCELL *et al.*, 1946]. In many Earth science applications, the hydrogen atom, associated with a water molecule, is the atom of interest. At the start of an NMR experiment on a geological material containing water, the nuclear spins associated with the hydrogen nuclei in the water of the pore space are at equilibrium in the presence of an applied, static magnetic field. In NMR logging applications, the applied static magnetic field is created by permanent magnets on the logging tool. The magnetic field results in a net magnetization that is proportional to the total number of spins within the pore space of the sampled material. An external oscillating magnetic field is then applied, causing the spins to rotate into the plane perpendicular to the background applied, static field. After perturbation, the spins return, or “relax,” to their initial state; during relaxation, the magnetization is measured. The relaxation is quantified in terms of two time constants: the relaxation time associated with the growth of the magnetization in the direction parallel to the background applied static field (T_1) and the relaxation time associated with the decay of the magnetization in the direction perpendicular to the background field (T_2). In this study, we employed an advanced acquisition mode that measured both time constants but chose to focus our analysis on the T_2 relaxation time because it is the superior measurement for short time

constants. Additionally, because T_1 relaxation is time consuming to measure, T_2 relaxation is more commonly measured in Earth science applications.

[9] In a single water-saturated pore, the total measured magnetization in the direction perpendicular to the background field (M) decays as a function of time (t) as a mono-exponential given by

$$M(t) = A_0 e^{-t/T_2}, \quad (1)$$

where A_0 is the amplitude of the magnetization at time zero and is proportional to the total number of spins, or volume of water, in the pore. The measured relaxation time, T_2 , is determined by the combination of two relaxation mechanisms, and can be expressed as

$$T_2^{-1} = T_{2B}^{-1} + T_{2S}^{-1}, \quad (2)$$

where T_{2B}^{-1} is the bulk fluid relaxation rate and T_{2S}^{-1} is the surface relaxation rate. There is an additional diffusion-related mechanism that contributes to the T_2 measurement and is due to gradients in the magnetic field. However, given the advanced data acquisition method used in this study for the NMR logging measurement, the equation above was adopted. Surface relaxation occurs due to interactions between the spins and the surface of the pore. In the case of fast diffusion, which assumes that all spins can diffuse (travel) to and relax at the pore surface during the time of the NMR experiment [Brownstein and Tarr, 1979], the surface relaxation rate is given by

$$T_{2S}^{-1} = \rho \left(\frac{S}{V} \right), \quad (3)$$

where ρ is the surface relaxivity, the ability of the pore wall to enhance relaxation, and (S/V) is the ratio between the total surface area and the total volume of void space of the single pore. In Earth science applications, it is commonly assumed that T_{2S}^{-1} dominates in (2), i.e., the contribution of T_{2B}^{-1} is negligible, so that in a single pore, we can assume that T_2^{-1} is equal to T_{2S}^{-1} .

[10] Porous geologic materials are not composed of a single pore, but rather, of many pores. In these water-saturated geologic materials, it is commonly assumed that a relaxing spin samples only a single pore so that each pore contributes to the NMR signal in isolation. Under this assumption, the measured magnetization is described as a multiexponential decay, interpreted to be the sum of the decays in each i th pore type, where a pore type is defined as having a specific (S/V) and ρ value. In most applications, it is assumed that ρ does not vary significantly within a sampled geologic material and can be assumed constant. In materials with a distribution of pore types, M decays as a multiexponential given by

$$M(t) = \sum_i A_i e^{-t/T_{2i}}, \quad (4)$$

where the amplitude, A_i , is proportional to the total number of spins, or the total volume of water, within the i th pore type, which relaxes with a relaxation time, T_{2i} . In

water-saturated materials, the sum of the A_i values is proportional to the total porosity within the sampled volume. If we again assume that T_{2S}^{-1} dominates and that ρ is constant throughout the material, i.e., that bulk relaxation is negligible, we can write each T_{2Si}^{-1} relaxation rate as

$$T_{2Si}^{-1} = \rho \left(\frac{S}{V} \right)_i, \quad (5)$$

where $(S/V)_i$ is the ratio between the total surface area and the total volume of void space of the i th pore type within the material.

[11] The multiexponential relaxation is typically displayed as a relaxation time distribution of A_i values versus T_{2i} . The fundamental assumption that each pore contributes to the NMR signal in isolation allows us to relate the T_{2i} distribution to a $(V/S)_i$ distribution through a simple linear transform (multiplication by ρ). Under this assumption, NMR data provide information about the amount of water that is contained in the i th pore type with a corresponding $(V/S)_i$ value. With the simplifying assumption of spherical pores, the $(V/S)_i$ distribution provides a pore size distribution. Finally, in addition to interpretation based on the complete relaxation time distribution, the T_2 distribution can be represented as a single value by taking the mean of the log of T_2 (T_{2ML}) given by [Brown and Fantazzini, 1993]

$$T_{2ML} = \exp \left(\frac{\sum A_i \ln(T_{2i})}{\sum A_i} \right). \quad (6)$$

[12] T_{2ML} is the single value representation of the T_2 distribution utilized in the SDR equation.

2.2. Link Between NMR Relaxation Measurements and Permeability

[13] Two equations used in petroleum applications to estimate permeability from NMR data, the SDR and T-C equations, are based on the Kozeny-Carman (K-C) relationship [Kozeny, 1927; Carman, 1956]. The K-C relationship predicts permeability (k_{K-C}) from porosity, ϕ , and the ratio between the total surface area and the total volume of void space (S_T/V_T) of the material, and can be written as follows [Gueguen and Palcaiuuckas, 1994]:

$$k_{K-C} = a \frac{\phi}{(S_T/V_T)^2}, \quad (7)$$

where a is a dimensionless constant that captures the tortuosity and shape of the pores within the material. This equation was modified for use with NMR logging data to include the measured T_2 relaxation time by replacing the (S_T/V_T) term with T_{2ML} and adjusting the exponent on porosity. Built on earlier work by SeEVERS [1966], permeability estimated from the SDR equation (k_{SDR}) is given by [Kenyon et al., 1988]

$$k_{SDR} = b \phi^m T_{2ML}^2, \quad (8)$$

where b and m are empirically determined constants that are interdependent. The porosity exponent, m , acts as a

weighting factor that can account for the amount of porosity that contributes to flow. It has been empirically determined through laboratory studies on consolidated materials to be 4 [Kenyon *et al.*, 1988]. It has been suggested that the increase in the porosity exponent from 1, in the original K-C relationship, to 4, better accounts for the contribution of pore throats, which are thought to control flow in consolidated materials. The empirical constant b , often termed the lithologic constant, captures the a term from the K-C relationship and an effective ρ . In petroleum applications, k_{SDR} estimates are provided in units of millidarcies (mD) with $T_{2\text{ML}}$ expressed in units of milliseconds (ms) so that b is provided in units of mD m s^{-2} . For an m value of 4, the constant b has been empirically determined through laboratory studies on consolidated sandstone materials to range from 4 to 5 mD m s^{-2} [Kenyon, 1997; Straley *et al.*, 1997]; in petroleum applications, the standard value is 4 mD m s^{-2} [Kenyon *et al.*, 1995]. To predict permeability in units of m^2 from $T_{2\text{ML}}$ given in units of seconds, the corresponding standard b value is $3.9 \times 10^{-9} \text{ m}^2 \text{ s}^{-2}$.

[14] As an alternative to replacing the (S_T/V_T) term in (7) with $T_{2\text{ML}}$, the T-C equation replaces the (S_T/V_T) term with the ratio between the free fluid index (FFI) and the bound volume index (BVI) [Timur, 1968, 1969a, 1969b; Coates *et al.*, 1991a, 1991b]. The FFI defines the amount of producible or extractable fluid within a sample, and the BVI defines the amount of water that is held in the pore space by capillary tension and/or clay-bound adsorption, which is related to the irreducible water saturation of the material. In the well, the amount of producible versus bound fluid will depend on the pumping rate and the induced pressure in the pore space. The “cutoff” time, the defined time that separates the FFI from BVI in the T_2 distribution, has been determined through laboratory studies on consolidated sandstone and carbonate samples. Although a range of cutoff times have been published, the cutoff times that have been adopted for use with consolidated sandstone and carbonate samples have been found to be 33 and 92 ms, respectively [Straley *et al.*, 1997], although the carbonate values vary widely. These times were determined by centrifuging the samples at 100 psi, which is typical of the pressure induced by pumping in petroleum applications. Permeability estimated from the T-C equation ($k_{\text{T-C}}$) is given by

$$k_{\text{T-C}} = c\phi^m \left(\frac{\text{FFI}}{\text{BVI}} \right)^2, \quad (9)$$

where k is in units of m^2 , and c and m are empirical constants that are interdependent and are specific to the 33 ms cutoff time. The empirical constant c , also termed the lithologic constant, captures the a term from the K-C relationship and an effective ρ , and can be expressed in units of m^2 . In petroleum applications, as with k_{SDR} estimates, $k_{\text{T-C}}$ estimates are provided in units of mD so that c is provided in units of mD. The constant c and has been empirically determined through laboratory studies on consolidated sandstone materials to be 1×10^4 mD [Allen *et al.*, 1988; Flaum *et al.*, 1998]. To predict permeability in units of m^2 , the corresponding standard value of c is $9.8 \times 10^{-12} \text{ m}^2$. As with the SDR equation, the porosity exponent m has

been empirically determined through laboratory studies on consolidated materials to be 4 [Coates *et al.*, 1991a, 1991b].

[15] In petroleum applications, it is common practice to obtain non-NMR-based estimates of permeability at discrete depths in order to calibrate the lithologic constants and determine cutoff times for each specific site [Hodgkins and Howard, 1999; Daigle and Dugan, 2009]; typically, the porosity exponent m is not modified. Sidewall cores can be obtained at depth using a logging tool that extracts cylindrical plugs perpendicular to the borehole. A petrophysical analysis, including obtaining estimates of porosity, permeability, and the cutoff time can be completed on the sidewall cores in the laboratory. Permeability estimates can also be obtained in the well using specialized logging tools, such as Schlumberger’s Express Pressure Tool (XPT). The XPT is a logging tool that provides estimates of permeability through analysis of pressure data. During data collection, the tool is pushed flush against the borehole wall, and a small port enters the formation, allowing a small amount of formation pore fluid to flow into the port. The tool measures the pressure in the formation as the system returns to equilibrium. The formation’s pressure profile can be interpreted for fluid mobility or permeability. The calibrated constants and determined cutoff time obtained at the laboratory scale on sidewall cores or at discrete depths in the borehole are then used to predict permeability at the field scale. Determining a set of calibrated empirical constants helps ensure reliable NMR-derived permeability estimates.

[16] In this study, we build on the decades of research completed in the petroleum industry to estimate permeability from NMR logging data in consolidated reservoirs and extend it to near-surface applications to estimate hydraulic conductivity in unconsolidated aquifers. There are, however, challenges that are encountered when working in near-surface materials. First, from a practical perspective, it can be very difficult to obtain hydraulic conductivity estimates at discrete depths through removal of sidewall cores and XPT logging. A field study by Maliva *et al.* [2009] noted that recovery of cores in aquifer materials was often poor and that intervals with the greatest hydraulic conductivity typically had the poorest recovery with cores often recovered as rubble. Plugs that are not recovered as perfect cylinders, or that cannot be cut into perfect cylinders, cannot be used in laboratory studies to obtain hydraulic conductivity estimates. Thus, in unconsolidated materials, it can be very difficult to extract sidewall cores that can be used to obtain hydraulic conductivity estimates. There are also likely to be problems obtaining reliable hydraulic conductivity estimates with the XPT. Irregular boreholes with increased rugosity can be expected to occur when drilling in unconsolidated materials; this makes it difficult to push the tool flush against the borehole wall. In addition, to ensure that the hydraulic conductivity measured with the XPT is representative of the in situ pore space, the formation surrounding the borehole should not be altered during drilling. In highly permeable zones, drilling mud creates a mud cake on the surface of the borehole and filtered fluid invades into the formation. If an inappropriate mud chemistry is used when drilling, or if invasion occurs too quickly, which is common in groundwater wells, the mudcake does not have time to form, and drilling mud can invade the

formation. In this scenario, the hydraulic conductivity estimate is not representative of the undisturbed formation pore space [Nascimento and Denicol, 1999].

[17] Second, from a theoretical perspective, there are additional challenges in unconsolidated materials associated with the assumed relationship between the NMR measurement and the pore-space geometry [James and Ehrlich, 1999]. The link between the relaxation time distribution and the pore size distribution is the basis for predicting permeability from NMR measurements. This link is based on three fundamental assumptions: (1) pores are small, so that relaxation occurs in the fast diffusion regime, (2) surface relaxation dominates (the contribution of bulk fluid relaxation can be neglected), and (3) pores are isolated, so that a spin relaxes in a single pore. In unconsolidated materials, one or all of these assumptions may be violated.

[18] Unconsolidated aquifer materials are commonly composed of sands and gravels, which may have pore spaces that are relatively large. When pores are larger than a critical size, the assumption of fast diffusion might not always be valid, and relaxation can occur in a regime termed the slow-diffusion regime. In the slow-diffusion regime, the dominant surface relaxation rate for a pore is proportional to the distribution of the squared S/V values of the pore space [Brownstein and Tarr, 1979], which will alter the equation needed to calculate NMR-derived permeability. Additionally, if pores are larger than some critical size, so that the bulk fluid and surface relaxation rates are similar, the contribution of bulk fluid relaxation should no longer be assumed negligible and must be accounted for when defining the relationship between T_2 and T_{2S} [Dlugosch et al., 2011; Dlubac and Knight, 2012]. If pores are not isolated, but rather well-connected, pore coupling can occur in which the spins can diffuse between more than one pore type during relaxation. When this occurs, the link from the T_2 distribution to pore geometry and permeability breaks down [Ramakrishnan et al., 1999; Grunewald and Knight, 2009, 2011]. In this study, as is typically done in petroleum applications, we chose to assume that relaxation occurs in the fast-diffusion regime, that surface relaxation dominates, and that pores are isolated and used equations (8) and (9) for calculating NMR-derived permeability. We wanted to determine whether the approach, well established for petroleum applications, would yield accurate estimates of hydraulic conductivity in the High Plains aquifer.

3. Field Experiment

3.1. Field Site

[19] The High Plains aquifer underlies eight states in the central United States and is primarily used for agricultural and domestic water needs [Cannia et al., 2006]. At the field site in Lexington, Nebraska, the High Plains aquifer consists of the upper Quaternary alluvium (Alluvial aquifer), the lower Tertiary Ogallala Formation, and the Arikaree Group (Ogallala aquifer) (Figures 1 and 2). Previous work at the site indicates that the unconsolidated alluvial aquifer is unconfined and extends from the depth of the water table (~ 3 m) to 24 m below land surface [Anderson et al., 2009]. An approximately 3 m thick aquitard separates the Alluvial aquifer from the deeper Ogallala aquifer. Below the aquitard, from 27 to 102 m below land surface, is the

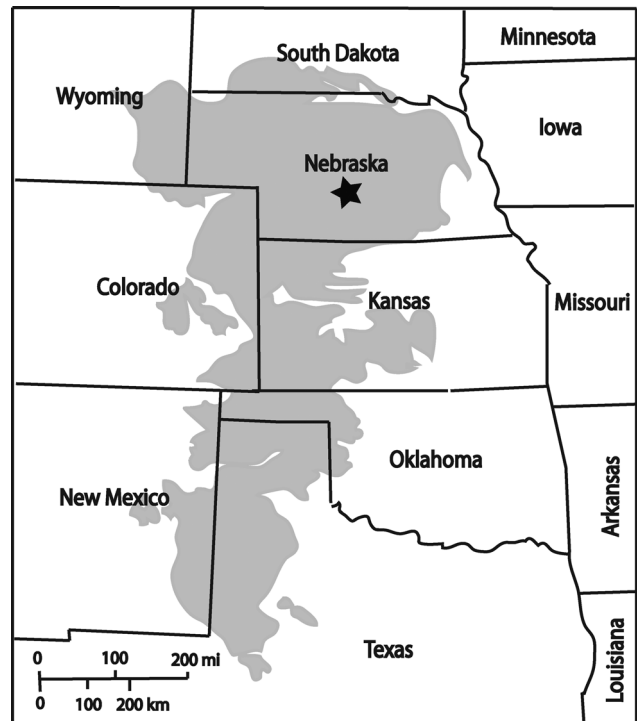


Figure 1. The High Plains aquifer (shown in gray) is located in the central United States [Kansas Geological Survey, 1993]. At the field site in Lexington, Nebraska, shown with a star, the High Plains aquifer consists of the upper Alluvial aquifer and the lower Ogallala aquifer.

unconsolidated to semiconsolidated, poorly sorted, gravel, sand, sandstone, silt, and clay of the Ogallala formation. Below the Ogallala formation, from approximately 102 to 133 m below land surface, is the unconsolidated to semiconsolidated, well-sorted, very fine-grained Arikaree Group. The Ogallala and Arikaree units form the leaky-confined Ogallala aquifer (Figure 2).

3.2. Geophysical Logging Data

[20] In the fall of 2009, a 24.5 cm diameter borehole was drilled to a depth of 128 m in the High Plains aquifer with a direct rotary drill using a water-based fluid with bentonite clay additives. Prior to casing the well, Schlumberger Water Services (SWS) acquired a suite of advanced geophysical logs. The suite of logs included NMR (MR Scanner), resistivity (Array Induction Imager, AIT), neutron porosity (Accelerator Porosity Sonde, APS), neutron-induced gamma ray spectroscopy (Reservoir Saturation Tool, RST), passive gamma (Hostile Environment Natural Gamma Ray Spectroscopy Tool, HNGS), and four arm caliper (Power Positioning Caliper, PPC). In this paper we focus on the interpretation of the NMR logging data.

[21] The NMR data were collected using the MR Scanner logging tool from 12 to 128 m depth. During data collection, the tool (10 m in length) is pushed against the borehole wall and samples a volume within a thin cylindrical shell (~ 3 – 4 mm in thickness) with about 100° of angular coverage at different depths of investigation (DOIs). In this study, two types of antennae were used: a main antenna with a frequency of 500 to 1000 kHz and a high-

Depth (meters)	Hydrostratigraphy	Lithology	Stratigraphy	Age
0-3	unsaturated zone	unconsolidated gravel, sand, and clay	Alluvium and eolian deposits	Quaternary
3-24	Alluvial aquifer			
24-27	aquitard	unconsolidated to semi-consolidated gravel, sand, sandstone, silt, siltstone, and clay	Ogallala Formation	Tertiary
27-102	Ogallala aquifer			
102-138		unconsolidated to semi-consolidated sand, silt, siltstone, and clay	Arikaree Group	

Figure 2. Depth, hydrostratigraphy, lithology, stratigraphy, and age of the High Plains aquifer at the field site in Lexington, Nebraska. Modified from *Anderson et al.* [2009].

resolution antenna with a frequency of 1,100 kHz. The main antenna had a vertical sample resolution of 45.7 cm, and data were collected at four DOIs: 3.8, 6.4, 6.9, and 10.2 cm. The high-resolution antenna had a vertical sample resolution of 19.1 cm, and data were collected at a DOI of 3.2 cm. The signal-to-noise ratio was improved by stacking the data, which resulted in a vertical support size of 1.83 m for data collected using the main antenna and 0.764 m for data collected using the high-resolution antenna. Data were then inverted using a Levenberg-based optimization to obtain diffusion-free distributions of T_1 and T_2 relaxation times and distributions of D , the diffusivity of the fluid, at each logged depth [Freedman and Heaton, 2004; Heaton et al., 2004]. In this study, we used the T_2 relaxation times for our analysis as they provide the best measurement of the short time constants, and measurements of long time constants, which are free from diffusion effects.

[22] We assessed which set of NMR logging data (antenna and DOI) most accurately represented the in situ formation conditions by estimating the amount of washout and whole mud invasion in the borehole. When significant washout occurs, there is danger that the NMR logging tool is not sampling the formation, but rather the bulk fluid, which in this case was drilling mud. The amount of washout can be quantified from the caliper tool, which measures the diameter of the borehole throughout the well. In this study, the caliper tool was only used during the first logging run (Figure 3, track 2) while the MR Scanner tool was used during the third through fifth logging runs. In unconsolidated materials, it is possible for the borehole wall diameter to change with each additional logging run. The caliper log showed that there was less than 10 cm of washout in most of the borehole but that significant washout occurred at several depths. By comparing the responses from the MR Scanner tool at different DOIs, it was found that the NMR data collected at 10.2 cm DOI was the most reliable in representing in situ formation conditions. The NMR T_2 distributions collected at 10.2 cm DOI along with the T_{2ML} values calculated using (6) are shown in Figure 3, track 4, as T_2 distributions (T_2 values versus amplitude). At this site, the T_{2ML} values ranged

from 2 to 820 ms. In general, we expect that lower T_{2ML} values will correspond to materials with higher S/V (e.g., clays or silts) and higher T_{2ML} values will correspond to materials with lower S/V (e.g., sands and gravels). The measured NMR porosity values ranged between 0.21 and 0.75 porosity units (P.U.) and are shown in Figure 3, track 5. We conclude that NMR data collected from 15 to 18 m depth, which have NMR-derived porosities over 0.5 P.U., were not representative of the in situ formation conditions and were affected by washout.

[23] Whole mud invasion also reduces the ability of the NMR logging tool to provide reliable measurements because the in situ formation fluids are altered. This affects the NMR measurement by pushing the relaxation times to smaller values [Nascimento and Denicol, 1999]. The extent of whole mud invasion was determined by examining the difference between the T_2 distributions collected from the deepest DOI (10.2 cm) and the two shallowest DOIs (3.8 and 6.4 cm). If whole mud invasion occurred, data collected at the shallowest DOI would most likely be affected and would show an increase in amplitude at low T_2 values compared to data collected at the deepest DOI, which would likely not have been affected and would represent the in situ formation conditions. Due to the effects of whole mud invasion during the drilling process, NMR data collected at a DOI of 10.2 cm were considered to have the highest data quality and were used for the analysis in this study.

[24] An integrated log analysis was used to model the mineralogy of the formation. The analysis was completed using the Elemental Log ANalysis (ELAN) program—a petrophysical interpretation program designed for depth-by-depth quantitative formation evaluation from borehole geophysical logs [Mayer and Sibbit, 1980; Quirein et al., 1986]. At this site, the data from the MR Scanner, RST, APS, and HNGS tools were used to perform the ELAN analysis. The ELAN results provided a volumetric estimate of the following minerals: quartz, calcite, orthoclase, montmorillonite, illite, and trace conductive minerals. The dry weight fractions of these minerals are shown in Figure 3, track 6.

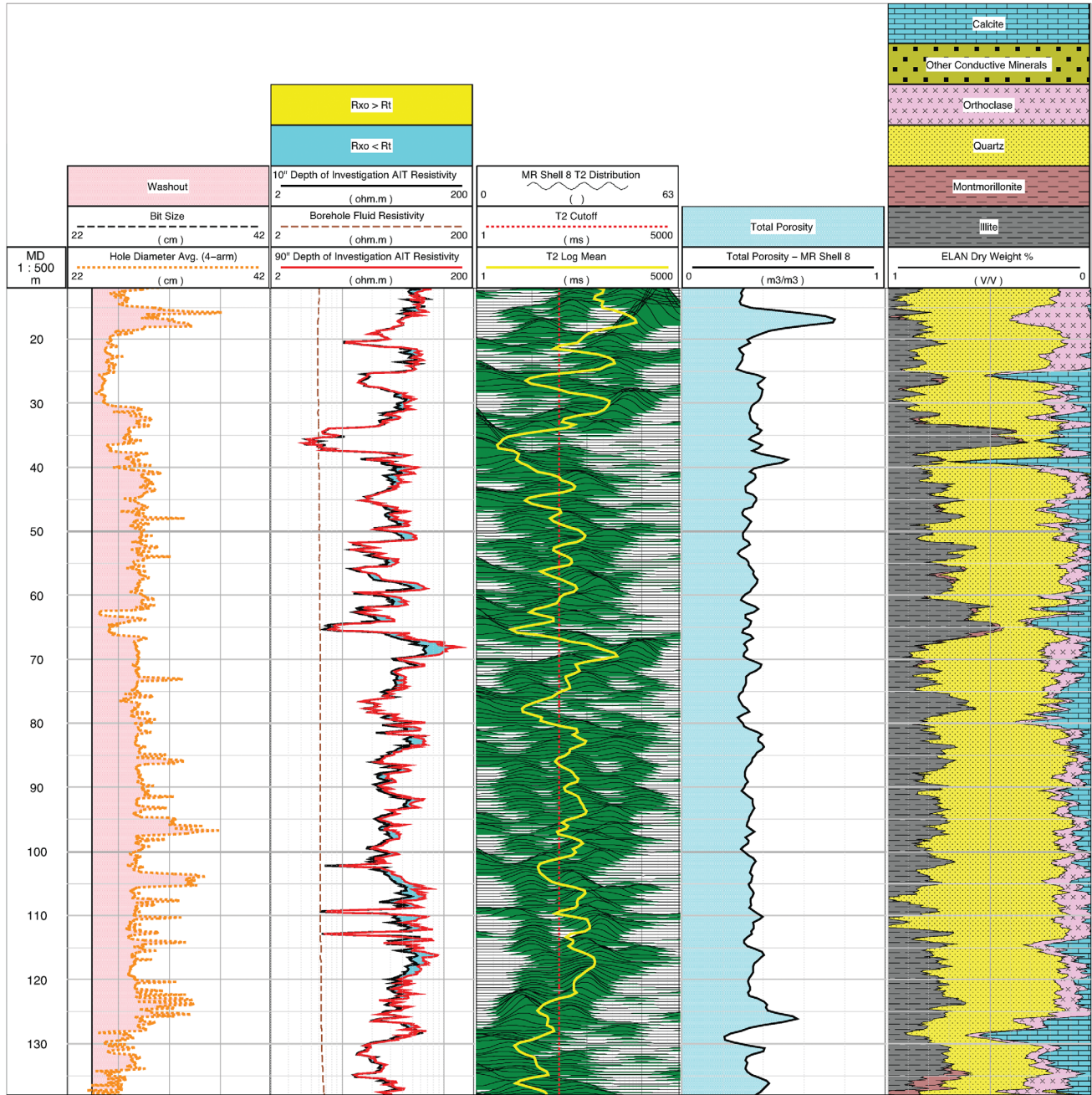


Figure 3. Track 1: Depth in meters. Track 2: Borehole geometry; average hole diameter in centimeters from PPC (orange dashed curve) with borehole washout/rugosity (pink shading). Track 3: Resistivity; bulk formation resistivity from AIT in ohmmeters at two DOIs—25 cm (solid black curve), 229 cm (solid red curve)—with the area between 229 cm and 25 cm resistivity curves shaded blue when the 229 cm DOI resistivity is greater than the 25 cm DOI resistivity and yellow when the 229 cm DOI resistivity is less than the 25 cm DOI resistivity. Track 4: NMR relaxation time distribution collected at 10.2 cm DOI with a support volume of 45.7 cm (waveforms); T_2 distributions recorded as normalized amplitudes (higher waveform peaks [green shading] corresponding to higher amplitude) versus logarithmic relaxation time (from 0.5 to 10,000 ms) with T_{2ML} (yellow curve) and T_2 distribution cutoff time of 33 ms (dashed red line). Track 5: NMR determined porosity. Track 6: Formation quantitative mineralogy (dry weight fraction); displays the results from the ELAN integrated log analysis presented as the dry-weight fractions of mineral types—illite clay (gray with long black hatches), montmorillonite clay (brown with short black hatches), quartz (yellow with small black dots), calcite (aqua blue with brick pattern), orthoclase or other potassium feldspar (lavender black cross hatches), and other conductive minerals (gold with large black dots).

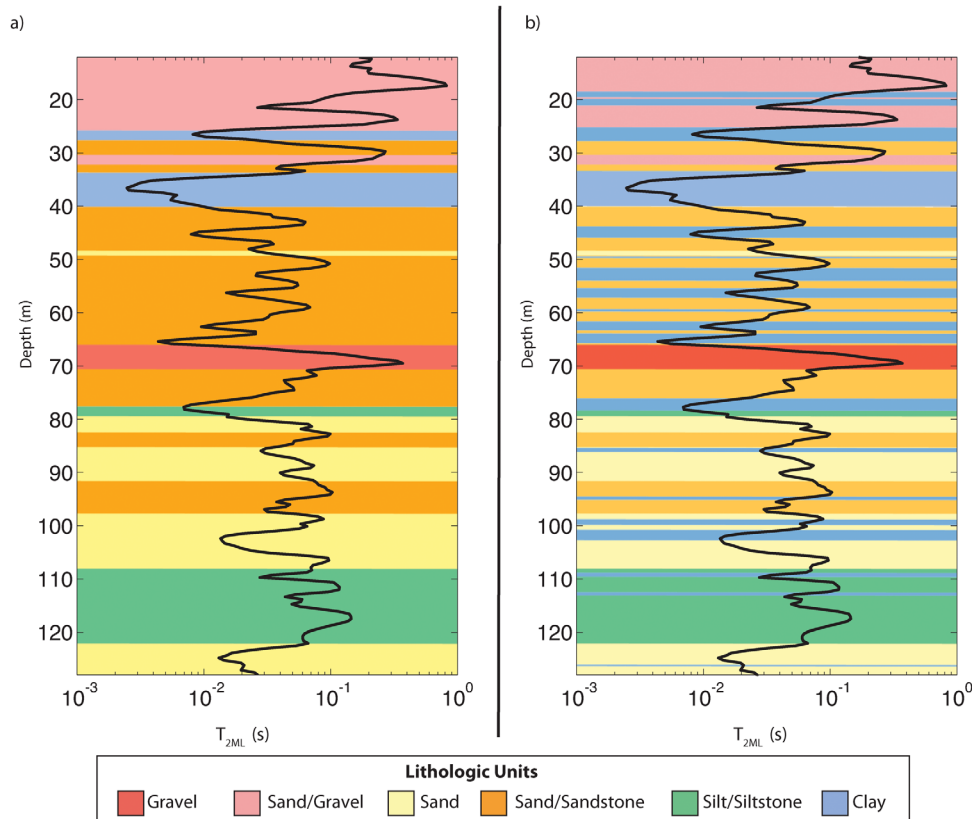


Figure 4. Lithology logs shown with NMR T_{2ML} values in seconds (solid black line). Generally, the clay layers correspond to low T_{2ML} values and the sands and gravels correspond to high T_{2ML} values. Lithologic units shown are gravel (red), sand/gravel (pink), sand (yellow), sand/sandstone (orange), silt/siltstone (green), and clay (blue). (a) The drill cuttings lithology log (DCLL) was likely not able to capture fine clay layers. (b) The refined lithology log, developed by integrating the resistivity log with the DCLL, shows more fine clay layers and corresponds well with the NMR T_{2ML} values.

3.3. Lithology Log

[25] During drilling, the drill cuttings were interpreted for lithology approximately every 1.5 m; this information was used to create a drill cuttings lithology log (DCLL). The DCLL is shown along with the NMR T_{2ML} values in Figure 4a. While we had confidence in the ability of the DCLL to identify the coarser-grained lithologic units (gravel, sand, sandstone, silt), we considered it very likely that clay layers were not captured in drill cuttings or were identified at incorrect depths. Due to the size of clay grains, it is possible to have the clay grains mix with the drilling mud, making them undistinguishable from the drilling mud. We used the resistivity log collected at the deepest DOI (2.29 m) (Figure 3, track 3) to identify clay layers missing from the DCLL. We decided to use the resistivity data collected from the deepest DOI as it was likely unaffected by invasion of the mud filtrate.

[26] Our approach was simple. We first “calibrated” the resistivity log by locating all clay units shown in the DCLL and determining the corresponding resistivity values. There was considerable variation in resistivity values that corresponded to the DCLL clay units. We found that, on average, the clay units corresponded to resistivity values less than $26 \Omega \text{ m}$. Therefore, at any depth where the resistivity log had a value less than $26 \Omega \text{ m}$, we defined the lithologic

unit to be clay or clay rich. At all other depths, we kept the lithology as identified in the DCLL. The final lithology log is shown with the NMR T_{2ML} values in Figure 4b. Generally, the clay layers defined in the final lithology log correspond to low T_{2ML} values and the sands and gravels correspond to high T_{2ML} values. Comparing the two lithology logs in Figure 4, the refined lithology log shows many fine clay layers that were missed in the drill cuttings and are not shown in the DCLL.

3.4. Hydraulic Conductivity Estimates for NMR Calibration

[27] In petroleum applications, it is common to obtain other estimates of permeability at discrete depths in order to calibrate the lithologic constants in the SDR and T-C equations. In this study, we obtained estimates of hydraulic conductivity using logging, laboratory, and hydrological methods. Schlumberger’s XPT was used to obtain discrete hydraulic conductivity estimates within the borehole. Twenty-four sidewall cores were extracted for laboratory analysis to determine hydraulic conductivity. Aquifer tests were completed to estimate transmissivity and average hydraulic conductivity in the Alluvial and Ogallala aquifers. WBF logging was completed to estimate the vertical

Table 1. Hydraulic Conductivity Estimates (m s^{-1}) Determined Through Logging, Laboratory, and Traditional Hydrological Methods^a

Depth (m)	Hydraulic Conductivity (m s^{-1})			
	XPT	SWC	Aquifer Test	WBF Logging
3				
6				
9				
12	8.0×10^{-8}			
15				
18				
21				
24				
27				
30				4.6×10^{-4}
34	1.5×10^{-8}	5.9×10^{-11}		
37				
40		5.1×10^{-11}		
43				1.1×10^{-5}
46		3.7×10^{-8}		
49		3.7×10^{-9}		1.8×10^{-5}
52		6.8×10^{-11}		
55				3.6×10^{-6}
58				
61				
64				
67	7.1×10^{-7}	1.4×10^{-10}		
70				3.2×10^{-5}
73		2.1×10^{-8}		
76				
79				2.9×10^{-5}
82				
85				7.2×10^{-6}
88	1.4×10^{-8}	7.6×10^{-9}		
91		6.4×10^{-9}		2.1×10^{-5}
94				
98				
101				
104				
107				
110		7.6×10^{-11}		
113				2.1×10^{-6}
116	7.3×10^{-7}			
119				
122		9.3×10^{-11}		
125				
128		3.8×10^{-9}		

^aColumn 1: Depth in meters. Column 2: Hydraulic conductivity estimates obtained from the XPT. Column 3: Hydraulic conductivity estimates obtained in the laboratory from constant head permeameter measurements on sidewall cores. Column 4: Hydraulic conductivity estimates obtained from aquifer test conducted in the Alluvial and Ogallala aquifers. Column 5: Hydraulic conductivity estimates obtained from WBF logging in the Ogallala aquifer.

distribution of transmissivity and hydraulic conductivity over the Ogallala aquifer.

[28] As a part of the SWS logging program, pressure data were collected using the XPT for use in calibrating the empirical constants in the SDR and T-C equations. Pressure data were collected at five discrete depths between 12 and 115 m and used to estimate in situ formation hydraulic conductivity (Table 1 and Figure 5).

[30] Sidewall cores were also collected as part of the SWS logging program using the Schlumberger Chronological Sample Taker (CST). Of the 30 requested sidewall cores, only 24 could be acquired; these were from specified

locations between the depths of 30.5 and 128 m. The CST is a percussion-type gun in which an electrically ignited powder-charge fires a hollow cylindrical bullet into the formation at each sample depth. Because the tool uses explosives to extract the cores, it was not within Schlumberger safety standards to obtain cores shallower than 30.5 m. The 24 acquired sidewall cores were individually wrapped in plastic wrap and placed in glass containers. The cores were then sent to a laboratory, where they were to be cleaned and hydraulic conductivity measured. Due to the lack of consolidation and near-wellbore formation damage, half of the cores had a noncylindrical shape, some were merely rubble, and were found unusable for hydraulic conductivity measurements. Only cores that could be cut into right cylinders could be used in the permeameter to obtain hydraulic conductivity measurements. Figure 6 shows an example of a sidewall core that was used to obtain hydraulic conductivity and an example of a sidewall core that was deemed unusable.

[31] Hydraulic conductivity was estimated on the sidewall core samples using a constant head permeameter, where a displacement pump was set upstream at a constant pressure and the flow rate through the sample was monitored. Once the flow rate and differential pressure across the sample were stable, hydraulic conductivity was calculated. The cores were assumed cleaned of any residual mud in the pore space during the time it took the samples to reach a constant flow rate and differential pressure. The hydraulic conductivity estimates obtained on the sidewall cores are listed in Table 1 and shown in Figure 5.

[32] In the spring of 2010, two 72 cm diameter wells were constructed at the field site and used to conduct aquifer tests; one test provided estimates of transmissivity and average hydraulic conductivity for the upper Alluvial aquifer and one test provided estimates of transmissivity and average hydraulic conductivity for the lower Ogallala aquifer. Each test was performed for 96 h with one pumping well and several observation wells. For the Alluvial aquifer test, the pumping well was drilled 7.5 m from the geophysical borehole to a depth of 24 m. The pumping well was completed with grout and gravel filter packs, screened from 12 to 24 m, and pumped at an approximate rate of $9.5 \times 10^{-2} \text{ m}^3 \text{ s}^{-1}$. Three observation wells were screened at depth intervals that spanned the pumped-well screen interval. The drawdown and recovery data were interpreted by curve fitting to a Moench solution [Moench, 1985] for an unconfined aquifer. The average hydraulic conductivity estimated for the Alluvial aquifer was $8.9 \times 10^{-4} \text{ m s}^{-1}$ (Table 1 and Figure 5). For the Ogallala aquifer test, the pumping well was drilled 10.5 m from the geophysical borehole to a depth of 128 m. The well was completed with grout and gravel filter packs, screened from 27 to 128 m, and pumped at an approximate rate of $8.7 \times 10^{-2} \text{ m}^3 \text{ s}^{-1}$. Eight observation wells were screened at depth intervals that spanned the pumped-well screen interval. The drawdown and recovery data were interpreted by curve fitting to a Moench solution for a leaky aquifer. The hydraulic conductivity calculated over the entire Ogallala aquifer was $3.7 \times 10^{-5} \text{ m s}^{-1}$ (Table 1 and Figure 5).

[33] Following the completion of aquifer tests, WBF logging data were collected with a Century Geophysical electromagnetic flowmeter in a 10 cm diameter well constructed at the field site. The well was constructed in a

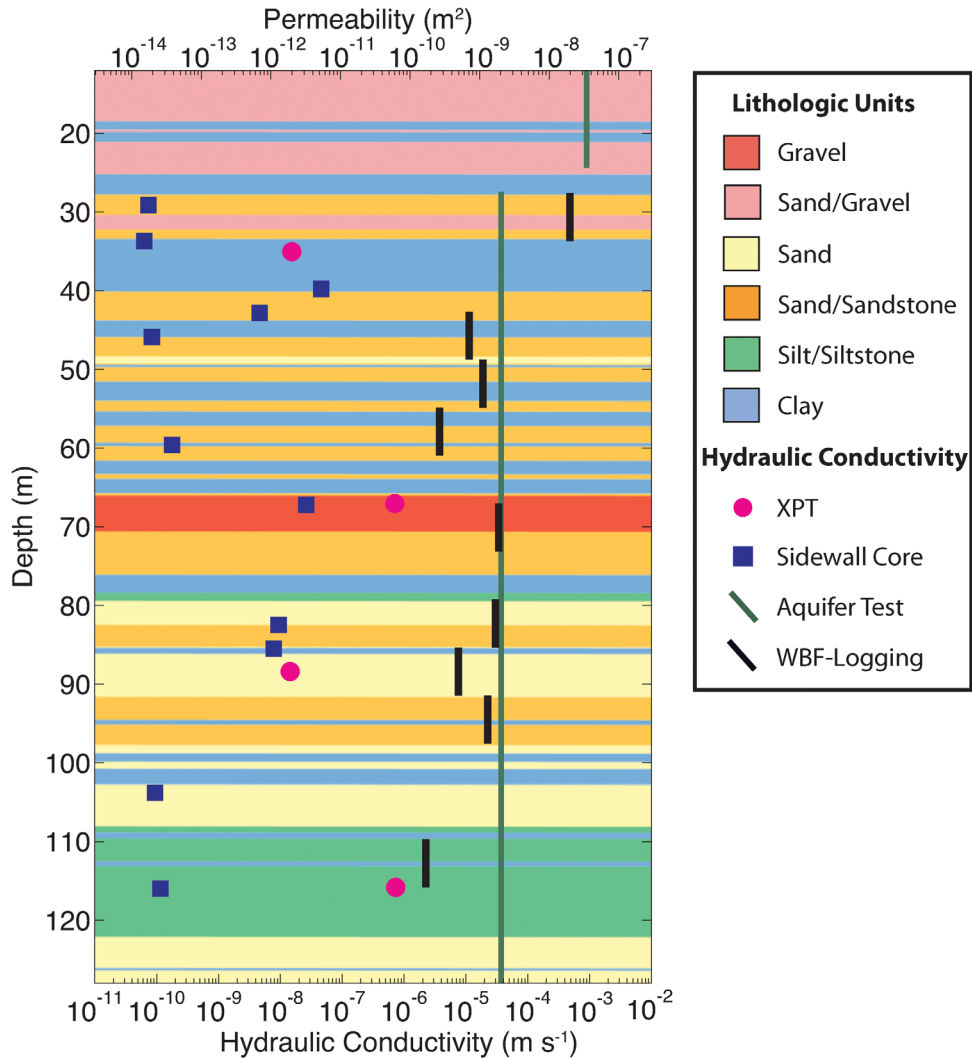


Figure 5. Hydraulic conductivity estimates determined from the XPT (pink dots), sidewall cores (blue squares), aquifer test (green line), and WBF logging (black line). Hydraulic conductivity in m s^{-1} shown on bottom x axis, permeability in m^2 shown on top x axis.

25 cm diameter borehole and was screened with gravel pack from 27 to 128 m below land surface. The WBF-logging method is able to detect flow zones whose transmissivity is within about 2 orders of magnitude of the most transmissive zone penetrated by the well. Flow through the gravel pack outside the well is not measured by the flowmeter. Data were collected in the Ogallala aquifer at approximately 6 m depth intervals under ambient and pumped conditions. Nine transmissive flow zones were detected by the WBF-logging method. The hydraulic conductivity of each of the nine zones was estimated from the WBF-logging data through the proportion method [Molz and Young, 1993]. The WBF-estimated hydraulic conductivity values (Table 1 and Figure 5) show a range from 3.5×10^{-6} to $4.6 \times 10^{-4} \text{ m s}^{-1}$.

4. NMR-Derived Hydraulic Conductivity Estimates

[34] The goal of our study was to determine the ability of NMR logging measurements to provide reliable estimates

of hydraulic conductivity in an unconsolidated aquifer. We first predicted hydraulic conductivity from NMR logging data using the SDR and T-C equations with the empirical constants determined for use with consolidated reservoir rocks. We compared the NMR-derived hydraulic conductivity (K_{NMR}) estimates to the other hydraulic conductivity estimates. We then optimized the fit between the WBF-logging hydraulic conductivity ($K_{\text{WBF-logging}}$) estimates and the K_{NMR} estimates to determine the empirical constants in the SDR and T-C equations for the materials of the High Plains aquifer at our field site.

[35] In order to compare K_{NMR} estimates determined using the SDR and T-C equations to $K_{\text{WBF-logging}}$ estimates, the high-resolution K_{NMR} estimates were upscaled to the resolution of $K_{\text{WBF-logging}}$ estimates. We made the fundamental assumption that because the borehole was fully screened throughout the producing zone of the aquifer, all flow into the well was horizontal flow. We could then assume that $K_{\text{WBF-logging}}$ estimates were horizontal hydraulic conductivity estimates. Under this assumption, the total horizontal hydraulic conductivity over an interval can be calculated as

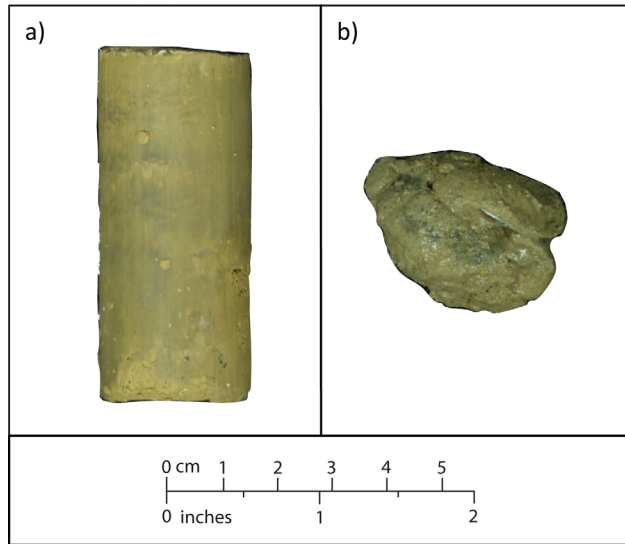


Figure 6. Examples of two sidewall cores obtained using the CST. Sidewall core (a) obtained at 35 m depth was used to obtain a hydraulic conductivity estimate. Sidewall core (b) obtained at 33.5 m depth was determined to be unusable by TerraTek to obtain a hydraulic conductivity estimate.

the arithmetic mean of the horizontal hydraulic conductivity of each layer within that interval. Within each of the nine WBF-logging intervals, upscaled K_{NMR} ($K_{\text{NMR-Upscaled}}$) estimates were calculated using the following:

$$K_{\text{NMR-Upscaled}} = \frac{1}{p} \sum_{i=1}^p (K_{\text{NMR}})_i, \quad (10)$$

where p is the number of NMR data with a vertical support size within the boundaries of the WBF-logging interval and p ranged from 12 to 13.

[36] We first calculated K_{NMR} using the SDR and T-C equations given in (8) and (9) with the standard empirical constants ($b = 3.9 \times 10^{-9} \text{ m}^2 \text{ s}^{-2}$, $c = 9.8 \times 10^{-12} \text{ m}^2$, $m = 4$) converted to provide estimates of hydraulic conductivity rather than permeability. Permeability is related to hydraulic conductivity through the following relationship [Freeze and Cherry, 1979]:

$$k = K \left(\frac{\mu}{\omega g} \right), \quad (11)$$

where g is gravity, and μ and ω are the dynamic viscosity and density of water, respectively, at a given temperature. To estimate hydraulic conductivity from the NMR data with $T_{2\text{ML}}$ expressed in seconds and K estimates provided in units of m s^{-1} , the corresponding SDR and T-C equations for a borehole temperature of 15°C are ($b = 3.4 \times 10^{-2} \text{ m s}^{-3}$, $c = 8.5 \times 10^{-5} \text{ m s}^{-1}$, $m = 4$)

$$K_{\text{SDR}} = 3.4 \times 10^{-2} \phi^4 T_{2\text{ML}}^2, \quad (12)$$

$$K_{\text{T-C}} = 8.5 \times 10^{-5} \phi^4 \left(\frac{\text{FFI}}{\text{BVI}} \right)^2. \quad (13)$$

[37] Figure 7a shows the continuous high-resolution K_{NMR} estimates determined using (12) and (13) along with

the corresponding $K_{\text{NMR-Upscaled}}$ estimates calculated using (10). Also shown are the XPT, sidewall core, aquifer test, and WBF-logging hydraulic conductivity estimates. At 45 m depth, K_{SDR} matches the hydraulic conductivity from the sidewall core. At all other depths, both K_{SDR} and $K_{\text{T-C}}$ overestimate the hydraulic conductivity from the sidewall cores by 1 to 2 orders of magnitude. Both K_{SDR} and $K_{\text{T-C}}$ agree with XPT hydraulic conductivity at depths of 33.5, 67, and 115 m. In four WBF-logging intervals, upscaled K_{SDR} estimates are 1 to 2 orders of magnitude less than $K_{\text{WBF-logging}}$ estimates; in five WBF-logging intervals, upscaled K_{SDR} estimates are within an order of magnitude of $K_{\text{WBF-logging}}$ estimates. In the WBF-logging interval from 110 to 116 m, the upscaled K_{SDR} estimate is within a factor of 2 of the $K_{\text{WBF-logging}}$ estimate. All of the upscaled $K_{\text{T-C}}$ estimates are within an order of magnitude of the $K_{\text{WBF-logging}}$ estimates; in six WBF-logging intervals, upscaled $K_{\text{T-C}}$ estimates are within a factor of 5 of $K_{\text{WBF-logging}}$ estimates.

[38] Given that there was such a large disagreement between the hydraulic conductivity predictions obtained from the XPT and sidewall cores, and the aquifer test and WBF-logging, the reliability of each hydraulic conductivity estimate was examined. Hydraulic conductivity estimates obtained from the XPT data and sidewall cores were orders of magnitude lower than the hydraulic conductivity estimates obtained from aquifer tests and WBF-logging. The XPT data were likely affected by either whole mud invasion into the formation or mud caking onto the formation wall, which can result in lowered hydraulic conductivity estimates. We also suspected that the sidewall cores had been invaded with mud and were not adequately cleaned before hydraulic conductivity estimates were obtained. Visual inspection of the cores confirmed whole mud invasion and showed distinct color variation across the core in several samples. It was concluded that hydraulic conductivity estimates obtained from the XPT and sidewall cores did not represent the in situ formation conditions due to whole mud invasion and were considered unusable for this study. We chose not to compare the K_{NMR} estimates to hydraulic conductivity estimates obtained through aquifer testing because the sample sizes were so different (centimeters versus tens of meters). We chose to compare $K_{\text{NMR-Upscaled}}$ to $K_{\text{WBF-logging}}$ estimates because they provided the most accurate hydraulic conductivity estimate with the highest resolution.

[39] As is common practice in the petroleum industry, we set the cutoff time in the T-C equation equal to 33 ms, then calibrated for the empirical constants in the SDR and T-C equations to determine a set of site-specific empirical constants that, we presumed, would be more appropriate for the unconsolidated and semiconsolidated materials of the High Plains aquifer. We determined the empirical constants by optimizing the fit between the $K_{\text{NMR-Upscaled}}$ and $K_{\text{WBF-logging}}$ estimates. We implemented a least-square inversion that minimized the root-mean-square error ($rmse$) of the logarithm of $K_{\text{NMR-Upscaled}}$ and the logarithm of $K_{\text{WBF-logging}}$ as shown below:

$$rmse = \sqrt{\frac{1}{q} \sum_{i=1}^q \left(\log(K_{\text{NMR-Upscaled}})_i - \log(K_{\text{WBF-logging}})_i \right)^2}, \quad (14)$$

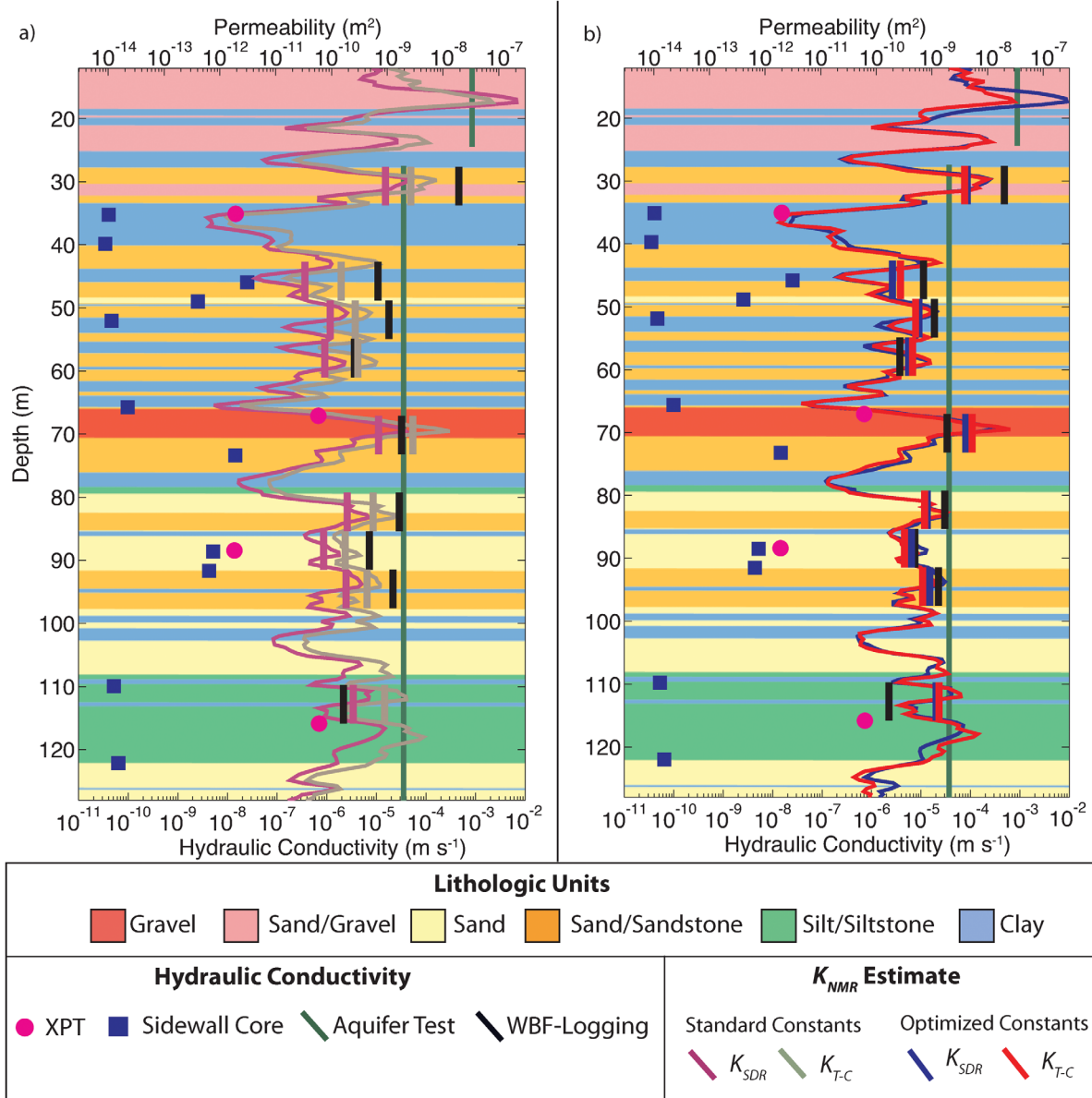


Figure 7. (a) NMR-derived hydraulic conductivity calculated using the SDR and T-C equations with the standard empirical constants and a cutoff time of 33 ms. The K_{SDR} estimates are shown in purple and the K_{T-C} estimates are shown in gray. The K_{NMR} estimates are upscaled so that they can be compared with $K_{WBF\text{-logging}}$ estimates. (b) NMR-derived hydraulic conductivity calculated using the SDR and T-C equations with the optimized empirical constants and a cutoff time of 33 ms. The optimized K_{SDR} estimates are shown in blue and the optimized K_{T-C} estimates are shown in red.

where q is the total number (9) of WBF-logging measurements. In addition to $rmse$, we also quantified error as the average error factor σ , given as

$$\sigma = 10^{(rmse)}, \quad (15)$$

and the average deviation, d , given as

$$d = \frac{1}{q} \sum_{i=1}^q |\log(K_{NMR})_i - \log(K_{WBF\text{-logging}})_i|. \quad (16)$$

[40] We used a semiconstrained least-square inversion to determine the empirical constants (b , c , and m) in the

T-C equation given in (8) and the SDR equation (9). We chose to constrain m , the exponent on porosity, to be positive, ranging from 0.5 and 8, increasing in value with an interval of 0.5; the lithologic constants b and c were unconstrained. The results for K_{NMR} estimates determined using the optimized empirical constants are shown in Figure 7b.

[41] The resulting optimized form of the SDR equation to predict permeability in units of m^2 with T_{2ML} provided in seconds is

$$k_{SDR} = 2.9 \times 10^{-9} \phi^2 T_{2ML}^2. \quad (17)$$

Table 2. Optimized SDR and T-C Equations to Predict Hydraulic Conductivity in Units of m s^{-1} With $T_{2\text{ML}}$ Provided in Seconds^a

Optimized K_{NMR}	<i>rmse</i>	σ	<i>d</i>
$K_{\text{SDR}} = 2.4 \times 10^{-2} \phi^2 T_{2\text{ML}}^2$	0.50	3.2	0.41
$K_{\text{T-C}} = 1.6 \times 10^{-5} \phi^2 (\text{FFI}/\text{BVI})^2$	0.54	3.5	0.48

^aQuantified error is given as the root-mean-square error (*rmse*) calculated using (14), average error factor (σ) calculated using (15), and average deviation (*d*) calculated using (16).

[42] The resulting form of the SDR equation to predict permeability in units of mD with $T_{2\text{ML}}$ provided in milliseconds, as is standard in petroleum applications, is

$$k_{\text{SDR}} = 2.9 \phi^2 T_{2\text{ML}}^2. \quad (18)$$

[43] The corresponding form of the SDR equation to predict hydraulic conductivity in units of m s^{-1} with $T_{2\text{ML}}$ provided in seconds is

$$K_{\text{SDR}} = 2.4 \times 10^{-2} \phi^2 T_{2\text{ML}}^2. \quad (19)$$

[44] The upscaled K_{SDR} estimates have *rmse*, σ , and *d* values of 0.50, 3.2, and 0.41, respectively (Table 2). All of the upscaled K_{SDR} estimates are within an order of magnitude of the $K_{\text{WBF-logging}}$ estimates (Figure 7b). In four WBF-logging intervals, upscaled K_{SDR} estimates are within a factor of 2 of the $K_{\text{WBF-logging}}$ estimates and in four WBF-logging intervals, upscaled K_{SDR} estimates are within a factor of 6 of the $K_{\text{WBF-logging}}$ estimates. Although the lithologic constant and porosity exponent are interdependent, we compare the values in (19) to those in (12) and find there is little change in the lithologic constant (which decreased only slightly) while the porosity exponent decreased from 4 to 2. This calibrated lithologic constant is slightly lower than the range of published values (3.9×10^{-2} to $4.2 \times 10^{-2} \text{ m s}^{-3}$) for lithologic constants in consolidated sedimentary materials [Chang et al., 1994; Kenyon, 1997; Straley et al., 1997]; published porosity exponents for consolidated sedimentary materials do not vary from 4. A sensitivity analysis of *b* and *m* showed that modifying *m* has a larger impact on the hydraulic conductivity estimate than modifying *b*. This suggests that hydraulic conductivity is more sensitive to changes in porosity than to changes in the lithologic constant. Because porosity is input as a fraction, the decrease in the porosity exponent suggests an increased dependence of the hydraulic conductivity on the NMR-derived porosity in these unconsolidated materials.

[46] The resulting optimized form of the T-C equation to predict permeability in units of m^2 is

$$k_{\text{T-C}} = 1.9 \times 10^{-12} \phi^2 \left(\frac{\text{FFI}}{\text{BVI}} \right)^2. \quad (20)$$

[47] The resulting form of the T-C equation to predict permeability in units of mD is

$$k_{\text{T-C}} = 1.9 \times 10^3 \phi^2 \left(\frac{\text{FFI}}{\text{BVI}} \right)^2. \quad (21)$$

[48] The corresponding form of the T-C equation to predict hydraulic conductivity in m s^{-1} is

$$K_{\text{T-C}} = 1.6 \times 10^{-5} \phi^2 \left(\frac{\text{FFI}}{\text{BVI}} \right)^2. \quad (22)$$

[49] The upscaled $K_{\text{T-C}}$ estimates have *rmse*, σ , and *d* values of 0.54, 3.5 and 0.48, respectively (Table 2). In only one WBF-logging interval, the upscaled $K_{\text{T-C}}$ estimate is an order of magnitude greater the $K_{\text{WBF-logging}}$ estimate (Figure 7b). In three WBF-logging intervals, upscaled $K_{\text{T-C}}$ estimates are within a factor of 2 of the $K_{\text{WBF-logging}}$ estimates and in the other five WBF-logging intervals, upscaled $K_{\text{T-C}}$ estimates are within a factor of 6 of the $K_{\text{WBF-logging}}$ estimates. We again compare the interdependent lithologic constant and porosity exponent in (22) to those in (13) and find that both the lithologic constant and the porosity exponent are decreased. Again, because porosity is input as a fraction, the decrease in the porosity exponent suggests an increased dependence of the hydraulic conductivity estimate on the NMR-derived porosity in these unconsolidated materials. It is interesting to note that the porosity exponent in both the calibrated T-C and SDR equations decreased from 4 to 2, which suggests consistency between the two equations and the contribution of the NMR-derived porosity to the calculation of hydraulic conductivity in these unconsolidated materials. There is little published on the range of values for the lithologic constant in the T-C equation, even for consolidated materials. Most of the research regarding site-specific calibrations to the T-C equation has been focused on determining appropriate cutoff times. In a field study, it is ideal to calibrate for the cutoff time using core samples as studies have shown that it can vary from 10 ms to over 100 ms, depending on the material [Borgia et al., 1991; Straley et al., 1991; Kenyon, 1992]. In this study, we did not determine the appropriate cutoff times using the sidewall cores because we believed they did not represent the in situ pore space due to whole mud invasion.

[50] A comparison of Figures 7a and 7b shows that optimizing for the empirical constants in the SDR equation provides drastically improved hydraulic conductivity estimates, while optimizing for the empirical constants in the T-C equation provides only slightly improved hydraulic conductivity estimates. In the WBF-logging interval from 110 to 116 m, the upscaled K_{SDR} estimate determined using the standard empirical constants is within a factor of 2 of $K_{\text{WBF-logging}}$, while the upscaled K_{SDR} estimate determined using the optimized empirical constants is almost an order of magnitude greater than $K_{\text{WBF-logging}}$. We note that this WBF-logging interval was located within the well-sorted, silt/siltstone and clay of the Arikaree unit while the other eight WBF-logging intervals were located within the poorly sorted, coarser grained Ogallala unit. It is possible that the surface relaxivity changed between these units, which would affect the NMR measurement and the resulting *K* estimate. In three WBF-logging intervals, from 55 to 61 m, 67 to 73 m, and 110 to 116 m, the standard empirical constants in the T-C equation provides more accurate upscaled $K_{\text{T-C}}$ estimates than the optimized T-C equation. There is no correlation between unit or lithology types in these WBF-logging intervals; one interval is located in an inter-layered sandstone/sand and clay section in the Ogallala unit, one interval is located in a gravel and sandstone/sand section in the Ogallala unit, and one interval is located in a

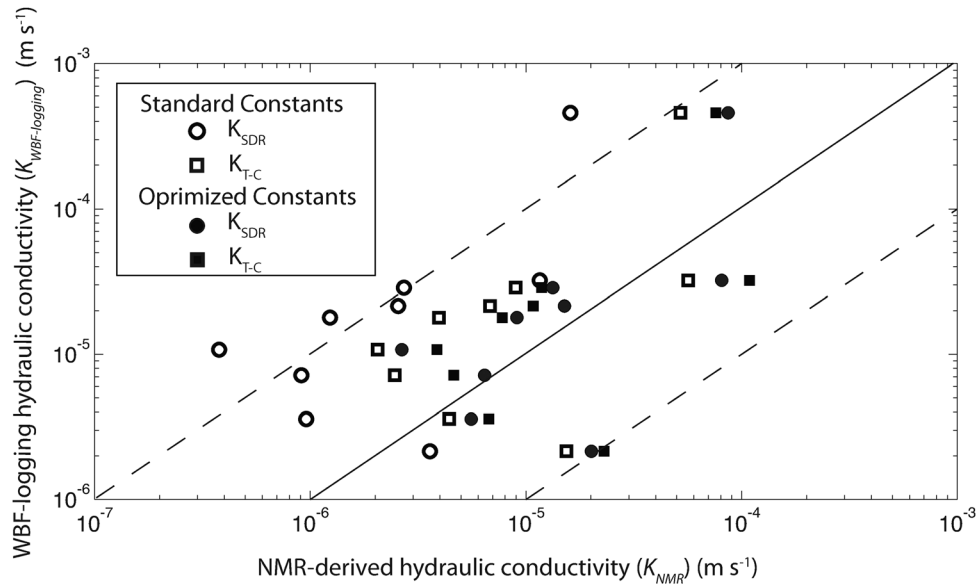


Figure 8. $K_{\text{WBF-logging}}$ estimates plotted versus the upscaled K_{NMR} estimates determined with the standard empirical constants in the SDR equation (12) shown as open circles and with the T-C equation (13) shown as open squares. Also shown are the upscaled K_{NMR} estimates determined with the optimized empirical constants in the SDR equation (19) shown as solid circles and with the T-C equation (22) shown as solid squares. The dashed lines show an order of magnitude greater and less than the one-to-one line.

silt/siltstone section in the Arikaree. In this study, because each WBF-logging interval included more than one lithology type, we could not determine lithology-specific empirical constants. We also note that a range of values for b , c , and m exist that provide K estimates that are within an order of magnitude of the true K . However, in this study, we determined the values for b , c , and m that provide the optimized fit between $K_{\text{NMR-Upscaled}}$ and $K_{\text{WBF-logging}}$.

[51] Figure 8 shows $K_{\text{WBF-logging}}$ estimates plotted against $K_{\text{NMR-Upscaled}}$ estimates. It can be seen that reliable hydraulic conductivity estimates (predicted within an order of magnitude of $K_{\text{WBF-logging}}$ estimates) can be obtained using the T-C equation with the standard cutoff time and empirical constants. We also show that by calibrating for the empirical constants in the SDR and T-C equations, we are able to provide reliable hydraulic conductivity estimates, the majority of which were within a factor of 5 of $K_{\text{WBF-logging}}$ estimates.

6. Conclusions

[52] In this study, we examined the ability of NMR logging measurements to provide reliable estimates of hydraulic conductivity in near-surface unconsolidated materials, where the success of a survey greatly depends on the quality and reliability of logging measurements. We encountered several problems in acquiring advanced geophysical logging data in the unconsolidated High Plains aquifer. We found that whole mud invasion occurred to varying degrees throughout the borehole. It may be possible to negate the effects of mud invasion in near-surface unconsolidated materials if water is used instead of mud or if a mud program is engineered for the specific geologic environment. Some of the main functions of drilling mud are to control

the formation pressure, maintain well stability, minimize formation damage, and cool the drill bit [Driscoll, 1986]. In shallow near-surface boreholes, controlling formation pressure and keeping the drill bit cool may be less of a concern than in petroleum applications. We also found that the amount of washout and rugosity in the borehole can be severe due to the unconsolidated nature of the formation; washout and rugosity can affect the near-wellbore data quality. Both of these conditions can become worse with each additional logging run, which suggests a need to log caliper data with each run. We also found little success with the removal of sidewall cores. At this site, half of the sidewall cores were removed as rubble and the hydraulic conductivity estimates from the remaining cores did not represent in situ formation conditions. In future near-surface studies in unconsolidated materials, sonic drilling [Barrow, 1994; Ruda and Farrar, 2006], which does not require the use of drilling mud, may be a better method for installing a borehole when the effects of mud invasion are a concern. The sonic drilling method applies high-frequency sound waves into a pipe, allowing for the pipe to penetrate the ground to depths of up to 250 m. Sonic drilling can also provide samples, although the pore geometry may be altered due to the vibrating pipe.

[53] We have shown that NMR logging can be used to provide reliable estimates of hydraulic conductivity in unconsolidated groundwater aquifers. We found that the use of standard empirical constants in the T-C equation provided hydraulic conductivity estimates that were within an order of magnitude of the $K_{\text{WBF-logging}}$ estimates. We optimized the fit between upscaled K_{NMR} and $K_{\text{WBF-logging}}$ estimates to determine a set of site-specific empirical constants that are likely more appropriate for the unconsolidated materials of the High Plains aquifer. At this site, the

optimized SDR equation provided lower residual errors than the optimized T-C equation. To our knowledge, this is the first use of NMR logging to estimate K in unconsolidated groundwater aquifers, and the first report of empirical constants determined specifically for unconsolidated near-surface materials.

[54] One obvious question arises from this study: How useful is NMR logging for estimating K if a calibration process is needed at each site? In petroleum applications, a set of standard empirical constants have been determined through decades of logging and laboratory studies, which are generally assumed to provide acceptable estimates of permeability. However, when a high level of accuracy is needed, other measurements of permeability are obtained, using either borehole or laboratory methods, in order to calibrate for the empirical constants. We anticipate that a similar approach will be used for hydrogeologic applications. This requires many more studies of NMR logging in groundwater systems to allow for the development of a database of empirical constants that can be used for estimating K in specific lithologies or aquifer units. If high accuracy in K is needed, then a more rigorous approach, like the one taken in this study, should be used to obtain a set of site-specific empirical constants. We conclude that with further research NMR logging will become widely adopted as a reliable method for obtaining estimates of K for hydrogeologic applications.

[55] **Acknowledgments.** This research was supported by funding to R. Knight and Y. Song from the Hydrology Program and the GOALI (Grant Opportunities for Academic Liaison with Industry) Program of the National Science Foundation (award 0911234); and by funding from the Central Platte Natural Resources District, Nebraska Environmental Trust, and the U.S. Geological Survey (USGS) Groundwater Resources Program. Any use of trade, firm, or product names is for descriptive purposes only and does not imply endorsement by the U.S. government. We wish to thank Duane Woodward, project hydrologist with Central Platte Natural Resources, for his support and assistance with the project. We thank Greg Steele and Chris Hozba from the Nebraska Water Science Center for describing drill cuttings and conducting aquifer tests; and thank Jim Geoke, University of Nebraska-Lincoln for describing drill cuttings and collecting continuous core. We also wish to thank John Keller from Terra-Tek for his assistance with the sidewall cores. Finally, we wish to thank the team of engineers from Schlumberger Wireline Services, Jared Hoskins, Kenan Noe, and Sam Hooper.

References

- Allen, D., G. Coates, J. Ayoub, J. Carroll, A. Borai, R. J. S. Brown, and D. Cannon (1988), Probing for permeability: An introduction to measurements, *Tech. Rev.*, 36, 6–12.
- Anderson, J. A., R. H. Morin, J. C. Cannia, and J. H. Williams (2009), Geophysical log analysis of selected test holes and wells in the high plains aquifer, Central Platte River basin, Nebraska, *U.S. Geol. Surv. Scientific Investigations Rep. (2009–5033)*, U.S. Geol. Surv., Reston, Va., p. 16.
- Barrow, J. C. (1994), The resonant sonic drilling method: An innovative technology for environmental restoration programs, *Ground Water Monitor. Remediat.* 14(2), 153–160.
- Bloch, F. (1946), Nuclear induction, *Phys. Rev.* 70(7-8), 460–473.
- Borgia, G. C., P. Fantazzini, and E. Mesini (1991), Wettability effects on oil-water-configurations in porous-media—A nuclear-magnetic-resonance relaxation study, *J. Appl. Phys.*, 70(12), 7623–7625.
- Brown, R. J. S., and P. Fantazzini (1993), Conditions for initial quasilinear T2-1 versus tau for Carr-Purcell-Meiboom-Gill NMR with diffusion and susceptibility differences in porous media and tissues, *Phys. Rev. B*, 47(22), 14823–14834.
- Brownstein, K. R., and C. E. Tarr (1979), Importance of classical diffusion in NMR studies of water in biological cells, *Phys. Rev.*, 19(6), 2446–2453.
- Butler, J. J. (1998), *The Design, Performance, and Analysis of Slug Tests*, 252 pp., Lewis Publishers, Boca Raton, Fla.
- Butler, J. J. (Ed.) (2005), *Hydrogeological Methods for Estimation of Spatial Variations in Hydraulic Conductivity*, 23–58 pp., Springer, Dordrecht, Netherlands.
- Butler, J. J., J. M. Healey, V. A. Zlotnik, and B. R. Zurbuchen (1998), The dipole flow test for site characterization: Some practical considerations (abstract), *EOS Trans. AGU*, 79(17), S153.
- Cannia, J. C., D. Woodward, and L. D. Cast (2006), Cooperative hydrology study COHYST: Hydrostratigraphic units and aquifer characterization report, The Cooperative Hydrology Study Group, p 96.
- Carman, P. C. (1956), *Flow of Gases Through Porous Media*, Academic, New York.
- Chang, D., H. Vinegar, C. Morriss, and C. Straley (1994), Effective porosity, producible fluid and permeability in carbonates from NMR logging, paper presented at SPWLA 35th Annual Logging Symposium, Soc. of Petrophys. and Well Log Anal., 19–22 June.
- Chen, C.-S., Y.-C. Sie, and Y.-T. Lin (2012), A review of the multilevel slug test for characterizing aquifer heterogeneity, *Terr. Atmos. Ocean Sci.*, 23(2), 131–143.
- Coates, G. R., M. Miller, M. Gillen, and G. Henderson (1991a), The MRIL in Conoco 33-1: An investigation of a new magnetic resonance imaging log, paper DD presented at SPWLA 32nd Annual Logging Symposium, Soc. of Petrophys. and Well Log Anal., 16–19 June.
- Coates, G. R., T. C. A. Peveraro, A. Hardwick, and D. Roberts (1991b), The magnetic resonance imaging log characterized by comparison with petrophysical properties and laboratory core data, paper SPE 22723 presented at SPE Annual Technical Conference and Exhibition, Soc. of Pet. Eng., Dallas, Tex., 6–9 October.
- Coates, G. R., L. Xiao, and M. G. Prammer (2000), *NMR Logging: Principles and Applications*, Halliburton Energy Serv., Houston, Tex.
- Daigle, H., and B. Dugan (2009), Extending NMR data for permeability estimation in fine-grained sediments, *Mar. Pet. Geol.*, 26(8), 1419–1427.
- Dlubac, K., and R. Knight (2012), A numerical study of the relationship between NMR relaxation and permeability in materials with large pores, paper presented at the 5th International Workshop on Magnetic Resonance, Hannover, Germany, 25–27 Sept.
- Dlugosch, R., M. Muller-Petke, T. Gunther, and U. Yaramanci (2011), An extended model for predicting hydraulic conductivity from NMR measurements, paper presented at Near Surface 2011, Euro. Assoc. of Geosci. and Eng., Leicester, U. K., 12–14 Sept.
- Driscoll, F. G. (1986), *Groundwater and Wells*, 1089 pp., Johnson Division, St. Paul, Minn.
- Dunn, K. J., D. J. Bergman, G. A. Latorraca (2002), *Nuclear Magnetic Resonance: Petrophysical and Logging Applications*, Elsevier, Oxford, U. K.
- Ellis, D. V., and J. M. Singer (2007), *Well Logging for Earth Scientists*, 2nd ed., 691 pp., Springer, Dordrecht, Netherlands.
- Flaum, C., R. L. Kleinberg, and J. Bedford (1998), Bound water volume, permeability, and residual oil saturation from incomplete magnetic resonance logging data, paper UU presented at SPWLA 39th Annual Logging Symposium, Soc. of Petrophys. and Well Log Anal., 26–29 May.
- Freedman, R., and N. Heaton (2004), Fluid characterization using nuclear magnetic resonance logging, *Petrophysics*, 45(3), 241–250.
- Freeze, R. A., and J. A. Cherry (1979), *Groundwater*, Prentice-Hall, Englewood Cliffs, N. J.
- Grunewald, E., and R. Knight (2009), A laboratory study of NMR relaxation times and pore coupling in heterogeneous media, *Geophysics*, 74(6), E215–E221.
- Grunewald, E., and R. Knight (2011), A laboratory study of NMR relaxation times in unconsolidated heterogeneous sediments, *Geophysics*, 76(4), G73–G83.
- Gueguen, Y., and V. Palciauskas (1994), *Introduction to the Physics of Rocks*, 294 pp., Princeton Univ Press, Princeton, N. J.
- Heaton, N. J., C. C. Minh, J. Kovats, and U. Guru (2004), Saturation and viscosity from multidimensional nuclear magnetic resonance logging, paper SPE 90564 presented at the presented at SPE Annual Technical Conference and Exhibition, Soc. of Pet. Eng., Houston, Tex., 26–29 Sept.
- Hodgkins, M. A., and J. J. Howard (1999), Application of NMR logging to reservoir characterization of low-resistivity sands in the Gulf of Mexico, *AAPG Bull.*, 83(1), 114–127.
- James, R. A., and R. Ehrlich (1999), Core-based investigation of NMR logging as a tool for characterization of shallow unconsolidated aquifers, *Ground Water*, 37(1), 48–57.
- Kabala, Z. J. (1993), The dipole flow test—A new single-borehole test for aquifer characterization, *Water Resour. Res.*, 29(1), 99–107.

- Kansas Geological Survey, K. G. W. (1993), Ground-water occurrence, in Kansas Geological Survey, Kansas Ground Water, Lawrence, Kansas. [Available at http://www.kgs.ku.edu/Publications/Bulletins/ED10/04_occur.html.]
- Kenyon, W. E. (1992), Nuclear magnetic resonance as a petrophysical measurement, *Nuclear Geophysics*, 6(2), 123–171.
- Kenyon, W. E. (1997), Petrophysical principles of applications of NMR logging, *Log Analyst*, 38(2), 21–43.
- Kenyon, W. E., P. Day, C. Straley, and J. F. Willemsen (1988), A three-part study of NMR longitudinal relaxation properties of water saturated sandstones, *SPE Form. Eval.*, 3, 622–636.
- Kenyon, W. E., C. Straley, P. N. Sen, M. Herron, A. Matteson, and M. J. Petricola (1995), A laboratory study of nuclear magnetic resonance relaxation and its relation to depositional texture and petrophysical properties—Carbonate Thamama group, Mubarraz Field, Abu Dhabi, paper SPE 29886 presented at SPE Middle East Oil Show, Soc. of Pet. Eng., Bahrain, 11–14 Mar.
- Kozeny, J. (1927), Ueber kapillare leitung des wasser im boden, *Wein Akad Wiss*, 136(2a), 271–307.
- Lewis, R. E., E. A. Clayton, and J. A. Goodrich (2000), Advanced geophysical logging technologies for aquifer characterization, paper presented at the International Conference on Groundwater, Fortaleza, Brazil.
- Maliva, R. G., E. A. Clayton, and T. M. Missimer (2009), Application of advanced borehole geophysical logging to managed aquifer recharge investigations, *Hydrogeol. J.*, 17(6), 1547–1556.
- Mayer, C., and A. Sibbit (1980), GLOBAL, A new approach to computer-processed log interpretation, paper SPE 9341 presented at SPE Annual Technical Conference and Exhibition, Soc. of Pet. Eng., Dallas, Tex., 21–24 Sept.
- Moench, A. F. (1985), Transient flow to a large-diameter well in an aquifer with storatice semiconfining layers, *Water Resour. Res.*, 21, 1121–1131.
- Molz, F. J., and S. C. Young (1993), Development and application of borehole flowmeters for environmental assessment, *Log Analyst*, 34(1), 13–23.
- Nascimento, J. D., and P. S. Denicol (1999), Anomalous NMR responses in highly permeable sandstone reservoirs: A case study, paper EE presented at SPWLA 40th Annual Logging Symposium, Soc. of Petrophys. and Well Log Anal., 30 May–3 June.
- Parra, J. O., C. Hackert, M. Bennett, and J. A. Collier (2003), Permeability and porosity images based on NMR, sonic, and seismic reflectivity: Application to a carbonate aquifer, *Leading Edge*, 22, 1102–1108.
- Purcell, E. M., H. C. Torrey, and R. V. Pound (1946), Resonance absorption by nuclear magnetic moments in a solid, *Phys. Rev.*, 69(1-2), 37.
- Quirein, J., S. Kimminau, J. LaVigne, J. Singer, and R. Wendel (1986), A coherent framework for developing and applying multiple formation evaluation models, paper DD presented at the SPWLA 24th Annual Logging Symposium, Soc. of Petrophys. and Well Log Anal., 9–13 June.
- Ramakrishnan, T. S., L. M. Schwartz, E. J. Fordham, W. E. Kenyon, and D. J. Wilkinson (1999), Forward models for nuclear magnetic resonance in carbonate rocks, *Log Analyst*, 40(4), 260–270.
- Ruda, T., and J. Farrar (2006), *Environmental Drilling for Soil Sampling, Rock Coring, Monitoring Well Drilling, Borehole Logging and Monitoring Well Installation*, Taylor & Francis Group, Boca Raton, Fla.
- Seevers, D. O. (1966), A nuclear magnetic method for determining the permeability of sandstones, paper L presented at the SPWLA 7th Annual Logging Symposium, Soc. of Petrophys. and Well Log Anal.
- Straley, C., C. E. Morriss, W. E. Kenyon, and J. J. Howard (1991), NMR in partially saturated rocks: Laboratory insights on free fluid index and comparison with borehole logs, paper CC presented at the SPWLA 32nd Annual Logging Symposium, Soc. of Petrophys. and Well Log Anal.
- Straley, C., D. Rossini, H. J. Vinegar, P. Tutunjian, and C. E. Morriss (1997), Core analysis by low-field NMR, *Log Analyst*, 38(2), 84–94.
- Timur, A. (1968), An investigation of permeability, porosity and residual water saturation relationships, paper presented at SPWLA 9th Annual Logging Symposium, Soc. of Petrophys. and Well Log Anal., 23–26 June.
- Timur, A. (1969a), Producibile porosity and permeability of sandstones investigated through nuclear magnetic resonance, *Log Analyst*, 10(1), 3–11.
- Timur, A. (1969b), Pulsed nuclear magnetic resonance studies of porosity, mobile fluid and permeability of sandstones, *J. Pet. Technol.*, 21(6), 775–786.
- Walsh, D. O., E. Grunewald, P. Turner, and I. Frid (2010), Javelin: A slim-hole and microhole NMR logging tool, *Fast Times*, 15(3), 67–72.